

# We are IntechOpen, the world's leading publisher of Open Access books Built by scientists, for scientists

6,900

Open access books available

186,000

International authors and editors

200M

Downloads

Our authors are among the

154

Countries delivered to

TOP 1%

most cited scientists

12.2%

Contributors from top 500 universities



WEB OF SCIENCE™

Selection of our books indexed in the Book Citation Index  
in Web of Science™ Core Collection (BKCI)

Interested in publishing with us?  
Contact [book.department@intechopen.com](mailto:book.department@intechopen.com)

Numbers displayed above are based on latest data collected.  
For more information visit [www.intechopen.com](http://www.intechopen.com)



---

# Thermodynamics Simulations Applied to Gas-Solid Materials Fabrication Processes

---

Elisabeth Blanquet and Ioana Nuta

Additional information is available at the end of the chapter

<http://dx.doi.org/10.5772/51377>

---

## 1. Introduction

The development and the design of materials and/or the processes of their fabrication are generally very time consumer and with expensive operations. Various methods of development can be conceived. Often, "empirical" approaches are adopted: the choice of the experimental parameters is established either on technological or commercial criteria, the optimization being the results of a "trial and error" approach, or on the results of design of experiments (DOE) approach targeted at a property of a material or a parameter of a very particular process. Another approach is to use process modeling: to simulate the process by a more or less simplified model. The modeling of gas-solid materials fabrication processes brings together several physical and chemical fields with variable complexity, starting from thermodynamics and/or kinetics studies up to the mass and heat transport coupled with databases and with thermodynamic and/or kinetics transport properties.

The objective of this chapter is to illustrate the interest areas computer-aided materials design and of processes optimization based on the thermodynamic simulation and giving some interesting examples in different domains. Databases as well as their necessary tools for the implementation of the thermodynamic calculations will be described.

The thermodynamic simulations of multicomponent systems contribute at two important points: the selection of the material and the optimization of the conditions of fabrication. In order to obtain a finely targeted product which meet specific functionalities, it is necessary to answer the following questions:

- what type of composition, quantity, and microstructure of the material allow to obtain such properties?
- it is possible to elaborate the material? By what process, with which reagent/ species and which operating conditions?
- is stable this material during a treatment in temperature, and under a given atmosphere?

- does this material react with its environment (substrate, oven, atmosphere)?

These questions are connected because the properties of the material, essentially conditioned by the microstructure of the final material, are going to depend on its chemical composition, to the process, to the operating conditions and on dimensions of the fabrication equipment.

The answers to these questions can be provided and shown from calculation of phase diagrams, evaluation of chemical reactions, calculation of equilibrium pressures, and from reaction diagrams.

## 2. Description of the methodologies

To evaluate equilibrium state, two possible approaches exist. The first one is to choose *a priori* a limited number of species and the simple chemical reactions which are susceptible to represent the studied process, and to estimate one or several most favorable reactions. It can be reminded the very classic use of the diagrams of Ellingham for the synthesis of metals from their oxides.

The second approach, more complex, is based on the analysis and the consideration of all the species belonging to the chemical system in the studied process.

The optimization procedure must have the following stages:

- The analysis of the system with the inventory of all the species reasonably susceptible to be present during the reactions taking place in the process.
- The construction of a consistent set of thermodynamic data for these species.
- The thermodynamic calculations at equilibrium of complex system
- The best representation of the results for the users

Thus, the thermodynamic calculations often give satisfactory results for processes which use high temperatures and residence time or reaction but for processes at low temperature, the kinetic factors must be not neglected. That is why the recent developments of thermodynamic softwares tend to include descriptions of phenomena of diffusion and reaction kinetics.

The thermodynamic approach gives the superior limit of possibilities of process (considering the reaction rates as infinite). It can be the only way of modeling for a complex system where the mechanisms of reaction and the kinetic data are badly known.

To include some dynamic aspects (mass transport) in the modeling, an approach which takes into account the evaluation of flows will be presented. It concerns applications where the total pressure is low (<10 Pa).

### 2.1. The analysis of the system

The analysis of the system consists in listing the following points: the range of temperature  $T$ , range of pressure  $P$  or of volume  $V$ , the duration of the process, the list of the reagent species,

the inventory of the components of the reactor and the nature of the atmosphere. For these last points, it means elaborating a list of all the compounds, the gaseous species, the elements and the solid solutions which result from the combination of the basic elements of the system.

This list is automatically generated thanks to interfaces with databases. However, it is advisable to make sure that the used database is very complete. As an example, the list corresponding to the chemical system Si-C-H-Ar (proceeded CVD (Chemical Vapor Deposition)) contains about sixty species – excluding the hydrocarbons  $C_xH_y$  where  $x>3$  [1].

## 2.2. Calculation of a thermochemical equilibrium

In a process reactor, at constant pressure, the balance is reached when the total free Gibbs energy function of the system is minimal (equation 1). To determine the nature and the proportion of the present phases at equilibrium, it is necessary to have the description of the energies of Gibbs of all these phases.

$$\frac{\Delta G}{RT} = \sum_{j=1}^{Ne} q_j \frac{\Delta G_j}{RT} \quad (1)$$

where  $q_j$  the number of moles of the species  $j$ ,  $G_j$  the molar free energy of Gibbs of the species  $j$ ,  $Ne$  total number of species.

The Gibbs energy can be described from the enthalpy ( $H$ ) and the entropy ( $S$ ):

$$G(T) = H(T) - T * S(T) \quad (2)$$

with

$$H(T) = \Delta H(298K) + \int_{298K}^T c_p(T) dT \quad (3)$$

$$S(T) = S(298K) + \int_{298K}^T \frac{c_p(T)}{T} dT \quad (4)$$

The necessary data are thus:  $C_p(T)$ ,  $\Delta H(298K)$ ,  $S(298K)$  and the data of possible phases transitions  $T_{trans}$ ,  $\Delta H_{trans}(T)$ .

Various formalisms are adopted for the analytical expression of the function  $C_p(T)$ . Among them, the formalisms of the SGTE (Scientific Group Thermodata Europe) [2] (equation 5) and of the NASA [3](equation 6) are :

$$c_p(T) = a + bT + cT^2 + \frac{d}{T^2} \quad (5)$$

$$c_p(T) = a + bT + cT^2 + dT^3 + eT^4 \quad (6)$$

where a, b, c, d, e are adjustable parameters.

So, it can be described analytically the Gibbs energy G for a stoichiometric compound (equation 7), for a gas (equation 8) and a solution phase (equation 9):

$$G(T) = A + BT + CT \ln T + DT^2 + ET^3 + \frac{F}{T} \quad (7)$$

$$G(T, P) = G(T) + RT \ln \frac{\bar{P}}{P_0} \quad (8)$$

$$\left. \begin{aligned} G(T, x) &= \sum_i G_i^{ref}(T) + G^{id}(T, x_i) + G^{excès}(T, x_i) \\ G^{id}(T, x_i) &= RT \sum_i (x_i \ln x_i) \\ G^{excès}(T, x_i) & \text{ described from a model} \end{aligned} \right\} \quad (9)$$

Besides, as neither the enthalpy nor the entropy can be described in an absolute way, a reference state must be used for these two functions of state. For the entropy, the adopted convention consists in taking a zero value at 0 K. In the case of the enthalpy, the most common convention is to choose the stable structure of the element at  $T = 298\text{K}$ , as standard reference state (e.g. Al fcc, Ti hcp,  $\text{O}_2$  gas ...). For the reference state,  $\Delta H(298\text{K})=0$  and  $S(0\text{K})=0$ .

As the reliability of the results of the thermodynamics simulation depends widely on the quality and on the consistence of the necessary data, it is advisable to attach an importance to the consistence of the available information: thermodynamics measurements, theoretical calculations, characterizations (X-ray diffraction, Environmental Scanning Microscopy), balance of phases (diagrams). In the Table 1 are given some experimental and theoretical techniques usually used to obtain the thermodynamic data.

The thermodynamic information are accessible in compilations of binary phases diagrams (for example Hansen [5], Elliot [6], Massalski [7]), ternary (Ternary Alloys [8]), or specialized journals (CALPHAD, Journal of Phase Equilibria, Intermetallics...), or tables (JANAF Thermochemical Tables [9], Barin [10], Gurvich [11]).

Today, most of data are available in international electronic databases. In Europe, the economic interest group "Scientific Group Thermodata Europe [12]" proposes common data bases for compounds, pure substances and for solutions. Also let us quote the "Coach" data bank ( more than 5000 listed species) proposed by Thermodata [1], well adapted to simulate gas/solid processes, the FACT bank (oxides/salts) proposed by the company GTT [13] and the Research Center in Calculation Thermodynamics [14], base TCRAS [15], bases NASA combustion [16], NIST [17].

	Experimental	Theory
$\Delta H(T)$	Calorimetry (dissolution)	Ab initio calculations Estimations : Miedema [4], analogy
$C_p(298K), S(298K)$	Temperature measurement at low temperature	
$C_p(T)$		Estimations : Neumann-Kopp law( $\Delta C_p=0$ for a condensed compound)
$C_p, S(T)$	Differential Scanning Calorimetry (DSC)	volume-specific heat capacity calculations
$G(T)$	Electromotive force, Mass Spectrometry (activity data, partial pressures at equilibrium)	
$T^{trans}, H^{trans}(T)$	Differential Thermal Analysis (DTA) Thermogravimetric analysis (TGA)	

**Table 1.** The classically used techniques to obtain the thermodynamic data

### 2.3. Calculations of complex equilibrium

The software of complex equilibrium is based on the minimization at constant temperature  $T$  of the Gibbs energy and constant pressure  $P$  (equation 1) or Helmholtz energy (equation 10), at constant volume:

$$\frac{\Delta F}{RT} = \sum_{j=1}^{Ne} q_j \frac{\Delta G_j}{RT} - \frac{P.V}{RT} \quad (10)$$

$q_j$  the number of moles of the species  $j$ .

The constraints of mass equilibrium of each present element in the chemical system expressed according to the number of atoms on the pure element  $i$  ( $C$  elements) are translated by the equation (11):

$$n_i = \sum_{e=1}^{Ne} q_e T_i^e \quad \text{with } i = 1 \dots C \quad (11)$$

where  $T_i^e$  represents the stoichiometry of the species  $e$  for the element  $i$ .

These  $C$  equations can be translated under the matrix shape (equation 12):

$$[n] = [T] * [q] \quad \text{with } Ne > C \quad (12)$$

There are multiple algorithms allowing this minimization. Various classifications were given, the most exhaustive having been supplied by Smith and Missen [18]. In a simple way, two

groups of algorithms can be distinguished: on one hand the methods of direct minimization, about zero order for the calculation of the function  $G$ , on the other hand, the methods of the first order based on the equality of the chemical potential which require the calculation of the function derivatives. These last ones also include the methods of second order, using among others the algorithm of Newton-Ralphson which is based on the second derivatives. It is necessary to note that the methods of the first order must be perfectly controlled because they can lead to a maximum instead of a minimum and consequently to a wrong result.

A method of the first group is described below: the matrix  $T$  is decomposed into a regular square matrix  $T_p$  of dimension  $C$  and a matrix  $T_d$  of dimension  $(C, N_e - C)$  such as:

$$[n] = [T_p][q_p] + [T_d][q_d] \quad (13)$$

The  $C$  species which constitute the matrix column  $q_p$  are called the “main species” because they are chosen among the most important species and have by definition a linear independent stoichiometry. The  $N_e - C$  remaining species of the matrix  $T_d$  is called “derived species” although they are chosen as variables from the minimization. So the  $N_e - C$  values  $q_d$  are given by the procedure of minimization,  $C$  values  $q_p$  is calculated by resolving the linear system:

$$[q_p] = [T_p]^{-1}[n] - [T_p]^{-1}[T_d][q_d] \quad (14)$$

An iteration of this method is divided into two steps. Firstly, the phase of exploration, every variable is modified by a value  $+$  or  $- h$ .

If  $X_{n-1}$  is the vector representing the variables after  $n-1$  iterations: the species  $i$  having a step  $h_i$  and  $G_i$  the value of the function

$$G_i^+ = \Delta G(x_1, x_2, \dots, x_{i-1}, x_i + h_i, x_{i+1}, \dots, x_v) \quad (15)$$

if  $G_i^+ < G_i$  either,

$$G_i^{++} = \Delta G(x_1, x_2, \dots, x_{i-1}, x_i + 2h_i, x_{i+1}, \dots, x_v) \quad (16)$$

or,

$$G_i^- = \Delta G(x_1, x_2, \dots, x_{i-1}, x_i - h_i, x_{i+1}, \dots, x_v) \quad (17)$$

When the exploration phase is ended, the next step is to move to the second algorithm phase where from the values of  $G^+$  and  $X_n^+$  issued from the exploration phase, we calculate  $X^{++} = X_{n-1} + (X_n^+ - X_{n-1})$  as well as the corresponding value  $G^{++}$  to obtain the optimal set [19]. To proceed the minimization procedure, a certain number of more and more friendly softwares are available commercially. It can be listed as example:

- « Gemini1/Gemini2 » [1]
- « FactSage » [14]

- « MTDATA » [20]
- « Thermocalc » [21]

### 3. Applications

Thomas [22], Bernard [23] and Pons [24] present few examples on CVD processes to illustrate the use of an a priori thermodynamic analysis. In the following paragraphs, it was chosen to show other few examples which evidence the help of thermodynamic modeling in industrial bottlenecks:

- Thermal stability of Metal-Organic Precursors used in CVD and ALD processes.
- Stability of SiC in H<sub>2</sub> atmosphere
- HfO<sub>2</sub> plasma etching
- SiO<sub>2</sub> PVD evaporation-condensation deposition process.

In the last two examples which correspond to processes operating at low pressure (<1 Pa), in addition to pure thermodynamic approach, a dynamic approach was presented which includes calculations of the major species flows.

#### 3.1. Microelectronics: Thermal stability of metal-organic precursors used in CVD and ALD processes

In the pursuit of smaller and faster devices manufacture, microelectronics industry scales down feature sizes and thus has to develop new materials and processes. Nowadays, organometallic precursors are widely used in ALD (Atomic Layer Deposition) and CVD (Chemical Vapor Deposition) deposition processes due to low deposition temperature (generally below 523 K). The objective of computational modeling for gaseous phase processes like ALD or CVD is to correlate the as-grown material quality (uniformity, growth rate, crystallinity, composition, etc) to general parameters such as growth conditions, reactor geometry, as well as local parameters that are actual flow, thermal fields and chemical kinetics at the solid/gas interface.

The gaseous precursors compounds used for the transport of the elements to be deposited by these processes have to meet several physicochemical properties requirements including relatively high volatility, convenient decomposition behavior and thermal stability. The tantalum organometallic precursor pentakis dimethylamino tantalum (PDMAT), remains an attractive solution for tantalum nitride films deposition. Unfortunately, information on physical and chemical behavior of this kind of precursor is scarce and namely species that are formed during vaporization and transported to the deposition chamber remain generally unknown. Thus, the knowledge of thermodynamics of these gaseous compounds could help in the understanding of the transport and growth mechanisms. Indeed, thanks to thermodynamics, it is possible to evaluate what evolves at equilibrium in the precursor source, in the input lines and in the deposition chamber where deposition reactions occur. To control, optimize and understand any ALD or CVD processes, thermodynamic simulations are very useful and therefore data should be primarily assessed.

### 3.1.1. Assessment of PDMAT thermodynamic data by mass spectrometry

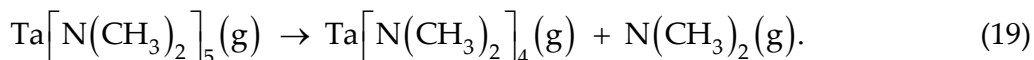
In order to deposit thin layers of TaN using PDMAT, ALD experiments evidenced a cracking of this precursor in the ALD reactor [25].

Cracking reactions of PDMAT can be complex and occur at the same time. A quantitative interpretation of cracking reactions can be deduced from observed molecules by mass spectrometry [26, 27] with the condition that all products and reactants of the reaction are observed and measured by the mass spectrometer at the same time. Without additional hydrogen contribution, the two following cracking reactions of Ta  $[\text{N}(\text{CH}_3)_2]_5(\text{g})$  could occur:

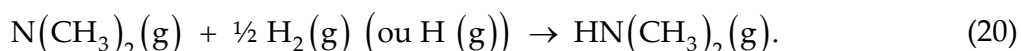
- i. either the Ta-  $[\text{N}(\text{CH}_3)_2]$  bond breaks with the additional break of H- $\text{CH}_2$  to produce  $\text{HN}(\text{CH}_3)_2$  (the so-called  $\beta$  substitution):



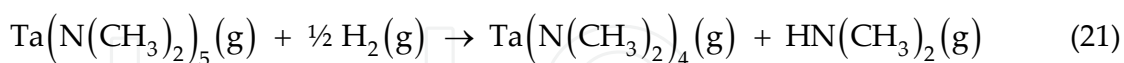
- ii. or the only bond break of Ta-  $[\text{N}(\text{CH}_3)_2]$ ,



As no  $\text{N}(\text{CH}_3)_2(\text{g})$  radical was detected, the observed  $\text{HN}(\text{CH}_3)_2(\text{g})$  molecule could be formed by the following complete and rapid reaction,



Consequently, it could be assumed that the measured  $\text{HN}(\text{CH}_3)_2(\text{g})$  amount is the same as the initial produced amount of  $\text{N}(\text{CH}_3)_2(\text{g})$ : this radical spontaneously reacts totally according to the reaction (20) after being produced by reaction (19). This mechanism could explain why  $\text{N}(\text{CH}_3)_2(\text{g})$  was not detected. So, in this study, the total cracking reaction was finally considered:



Another cracking reaction could be noticed:  $\text{OTaN}_4\text{C}_8\text{H}_{24}(\text{g})$  molecule broke down into  $\text{OTaN}_3\text{C}_6\text{H}_{18}(\text{g})$  according to the following reaction,



because the energy of the Ta-N bond is lower than the Ta-O bond.

The experimental study of these two reactions (21) and (22) requires to know or measure  $\text{H}_2(\text{g})$  pressure. Hydrogen could come from either equilibrium with cracking cell deposits or either molecules losing one or more hydrogen atoms. In this last case, a new molecule should be present. In this study, as no hydrogen was detected or introduced intentionally in the cell, it was assumed that the amino radical is totally consumed and produces  $\text{HN}(\text{CH}_3)_2(\text{g})$  with just a sufficient hydrogen amount. So, it can be assumed that the partial pressure of

$p(\text{HN}(\text{CH}_3)_2)$  is quite equal to the partial pressure of  $p(\text{N}(\text{CH}_3)_2)$ . That allows us to calculate the equilibrium constant of reaction (19):

$$K_p(T) = \frac{p(\text{N}(\text{CH}_3)_2) \cdot p(\text{Ta}[\text{N}(\text{CH}_3)_2]_4)}{p(\text{Ta}[\text{N}(\text{CH}_3)_2]_5)} \quad (23)$$

Pressure measurements of these three molecules by mass spectrometry lead to the evaluation of standard enthalpy at 298 K from the third law of thermodynamics:

$$\Delta_r H_{298\text{K}}^0 = -RT \ln K_p(T) - T \cdot \Delta_r fef_T^0 \quad (24)$$

Measured partial pressures of  $\text{Ta} [\text{N}(\text{CH}_3)_2]_5$  (g),  $\text{Ta} [\text{N}(\text{CH}_3)_2]_4$  (g) and  $\text{HN}(\text{CH}_3)_2$  (g) are elsewhere reported [26, 27].

From this, the average value of  $\Delta_r H_{298\text{K}}^0$  was evaluated to be equal to  $(85 \pm 5)$  kJ/mol.

### 3.1.2. Thermodynamic simulation of PDMAT (thermal cracking)

Thermodynamic simulations, based on the Gibbs free energy minimization of the Ta-C-N-H-(O)-(Ar) system were performed using GEMINI software [1] to provide the nature of the species that should be present at equilibrium under experimental conditions. The sets of thermodynamic data which have been used come from SGTE 2007 database [28] and from the mass spectrometry study for  $\text{Ta} [\text{N}(\text{CH}_3)_2]_5$ (g),  $\text{Ta} [\text{N}(\text{CH}_3)_2]_4$ (g), and  $\text{NC}_2\text{H}_6$  (g) gaseous species [26]. Without any available literature data or any estimates, it cannot be considered any thermodynamic description of  $\text{OTa}_n\text{C}_m\text{H}_z$  (g) gaseous species and intermediate  $\text{Ta}_n\text{C}_m\text{H}_z$  (g) species such as  $\text{Ta}_3\text{C}_6\text{H}_{16}$  (g), even though these species are expected to appear as observed in mass spectrometric measurements and to play a role in PDMAT cracking and in Ta containing solid formation [26]. Two kinds of simulations have been performed within a temperature range from 400 to 750 K and at 10 Pa, which is our typical mass spectrometric total pressure in the cracking cell. First, homogeneous equilibrium was investigated - no solid phase is allowed to be formed - which corresponds to no deposition i.e. transport in gas lines held at temperature above the saturated one (Figure 1).

Second, a heterogeneous equilibrium - the solid phase is allowed to be formed - has also been simulated, which corresponds to the deposition process occurring in the ALD reactor and in the cracking cell.

In all these thermodynamic simulations, it appeared that  $\text{Ta} [\text{N}(\text{CH}_3)_2]_5$ (g), (PDMAT) is not stable. In Figure 1 the homogeneous equilibrium calculation show that  $\text{Ta} [\text{N}(\text{CH}_3)_2]_4$ (g) is stable but disappears after 450 K and  $\text{Ta}$ (g) is the only one main tantalum containing species after 415 K - but this species will soon be condensed due to large over saturation-. Added to  $\text{Ta}$ (g), a lot of cracking gaseous species such as  $\text{N}_2$  (g),  $\text{CH}_4$  (g),  $\text{H}_2$  (g) originate from the complete amine decomposition and indeed among these species,  $\text{NC}_2\text{H}_7$  (g) and  $\text{NC}_2\text{H}_6$  (g)

do not appear. The heterogeneous equilibrium calculations shows the formation of C solid that corresponds to the amine decomposition and this amount of free carbon increases with increasing temperature. Also, the formation of solid TaN was observed within the whole investigated temperature range and no gaseous tantalum containing species pertained contrary to mass spectrometric experiments.

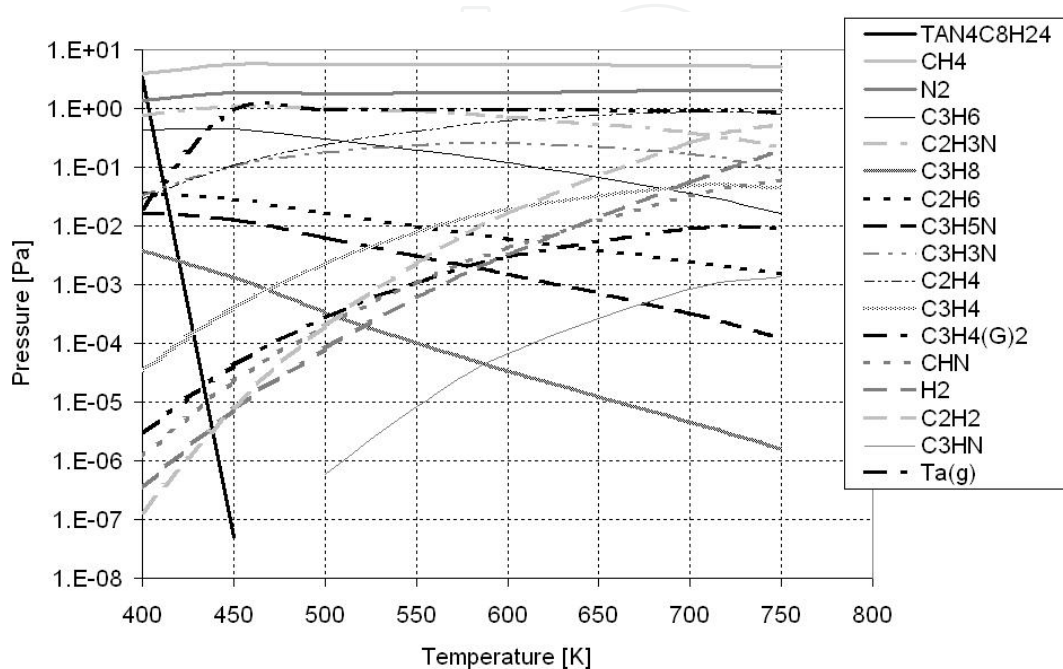


**Figure 1.** Homogeneous thermodynamic simulations performed starting from 1 mole of the compound Ta  $[\text{N}(\text{CH}_3)_2]_5(\text{g})$  and 0.001 mol of Ar and for an applied total pressure equal to 10 Pa in order to be compared with the mass spectrometric experiments.

### 3.1.3. Conclusions

It is to be concluded that discrepancies exist between thermodynamic simulations and mass spectrometric experiments. Indeed, thermodynamics predicted total cracking of both Ta  $[\text{N}(\text{CH}_3)_2]_5(\text{g})$  and amine molecules in the whole investigated temperature ranges, while in mass spectrometric experiments, Ta  $[\text{N}(\text{CH}_3)_2]_5(\text{g})$  and  $\text{NC}_2\text{H}_7(\text{g})$  amine have been observed only in the low temperature below 623 K [26, 29]. The deviation vs. equilibrium could be analyzed experimentally by the use of various sizes of cracking cell as well as the deliberate and controlled introduction of  $\text{H}_2(\text{g})$ . However, despite these limitations, these results indicate the main features of the precursor thermal behavior which can be very useful in the first stages of the development of any new ALD or CVD (for precursor transport) processes.

## 3.2. High power electronics: Stability of SiC in $\text{H}_2$ atmosphere

Silicon carbide (SiC) possesses many favorable properties making it interesting for a multitude of applications, from high temperature to high frequency and high power device.

Among them, its excellent physico-chemical and electronic properties such as wide band gap and high breakdown field, together with the degree of maturity of technology, makes SiC a good candidate for mass production of Schottky diodes [30].

SiC device processing is conditioned to the fabrication of large area single crystal wafers with the lowest defect density associated to deposition of epitaxial thin films which present good structural quality and controlled doping level [31]. The most common processes used to develop SiC wafers and SiC thin films are the seeded sublimation growth technique so called the "Modified Lely method" and the Chemical Vapor Deposition technique from propane and silane, respectively.

Huge improvements for both processes have been observed in the last decades. They come mainly from extensive experimental effort, all over different groups in the world. However, macroscopic modeling has given valuable information to understand the impact of some growth parameters and propose new design of experiment to enlarge wafer size and deposition area.

On both processes [32-35], some modeling trends were largely reported combined with experimental results obtained in our research's groups.

Special emphasis is given to chemical related results. To carry out modeling, it was followed the different levels of complexity procedure described in the earlier paragraphs. Owing to the similarity of the two systems, studies on species and material databases have been naturally used for both processes.

CVD- grown SiC films can be obtained from a variety of precursors which are generally part of the Si-C-H system. However, to obtain high crystal quality of 4H and 6H SiC layers, which are the most interesting polytypes for the power devices applications, experimental investigations have demonstrated that silane ( $\text{SiH}_4(\text{g})$ ) – propane ( $\text{C}_3\text{H}_8(\text{g})$ ) gave the most stable growth, in the typical conditions (temperature higher than 1700K, pressure between 10 kPa to 100kPa, hydrogen as carrier gas) [36]. Operations are separated in two steps, first an in situ etching step to prevent epitaxy-induced defects, then the deposition step.

A great body of literature dealing with both theoretical and experimental results has been devoted to understanding chemistries relevant to the separate Si-H and C-H systems.

However, it appears that most is unknown about the chemical reactions in which organosilicon species, that include the three elements, can be involved. This is related to the difficulty to measure thermochemical properties of such reactive, short life time, species. Most of the thermodynamic data that have been used for these species come from ab initio electronic structure calculations combined with empiric bond additivity corrections [37, 38]. Mass spectrometry measurements have been carried out to estimate the thermodynamic data of the gaseous species  $\text{Si}_2\text{C}(\text{g})$ ,  $\text{SiC}_2(\text{g})$ ,  $\text{SiC}(\text{g})$  and the condensed  $\text{SiC}(\text{s})$  phase [39, 40].

With a purely thermodynamic approach, it was examined the preliminary operation of in situ etching. It was found that the  $\text{H}_2(\text{g})$  etching of  $\text{SiC}(\text{s})$  at 1700 K under 100 kPa can lead to the formation of a condensed silicon phase, as shown on Figure 2. Thermodynamic study was made to understand the impact of the temperature, the pressure and the composition of the gas mixture [41].

Heterogeneous thermodynamic calculations show that the mixture ( $\text{H}_2(\text{g})$  + condensed  $\text{SiC}(\text{s})$ ) ends in the formation of gaseous species such as  $\text{CH}_4(\text{g})$  for the C-containing species and  $\text{SiH}_2(\text{g})$ ,  $\text{SiH}_4(\text{g})$ ,  $\text{SiH}(\text{g})$ ,  $\text{Si}(\text{g})$  and  $\text{Si}(\text{s})$  in condensed phase for the Si-containing species. With the etching, the amount of the gaseous C-species formed (mainly  $\text{CH}_4(\text{g})$ ) is three times higher than the gaseous Si-species one. So, there is Si in excess which is condensed at the  $\text{SiC}(\text{s})$  surface in a solid or liquid phase depending whether the etching temperature is higher or below the Si melting temperature. When the temperature is higher than 1800K, at atmospheric pressure, the quantity of formed gaseous Si-species becomes equal to the quantity of formed gaseous C-species. Consequently, the formation of liquid silicon is avoided.

### 3.2.1. Conclusions

Thermodynamic simulations have revealed the main phenomena and indicated some solutions. Reducing pressure would provide the same beneficial effect, though the etching rate decreases, as illustrated in Figure 3.

To compensate the formation of gaseous  $\text{CH}_4(\text{g})$ , the addition of an hydrocarbon species such as propane in the initial gaseous mixture would prevent the formation of condensed silicon.

All these effects have been confirmed with experimental studies (Figure 2).

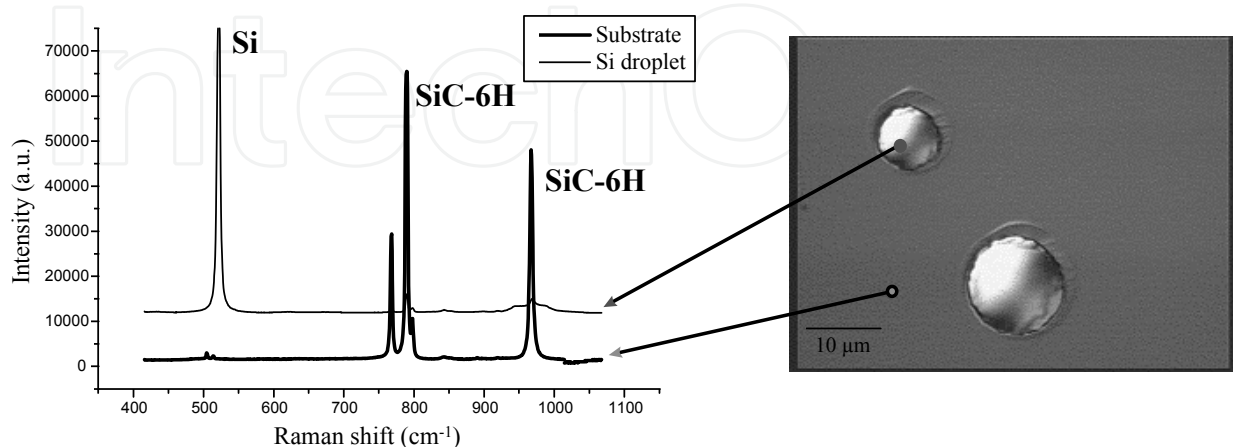


**Figure 2.** Optical Micrograph of  $\text{SiC}(\text{s})$  surface etched with  $\text{H}_2(\text{g})$  at 1700 K under 100 kPa, showing silicon droplets (right). The silicon phase is identified by Raman spectroscopy (left) [41].

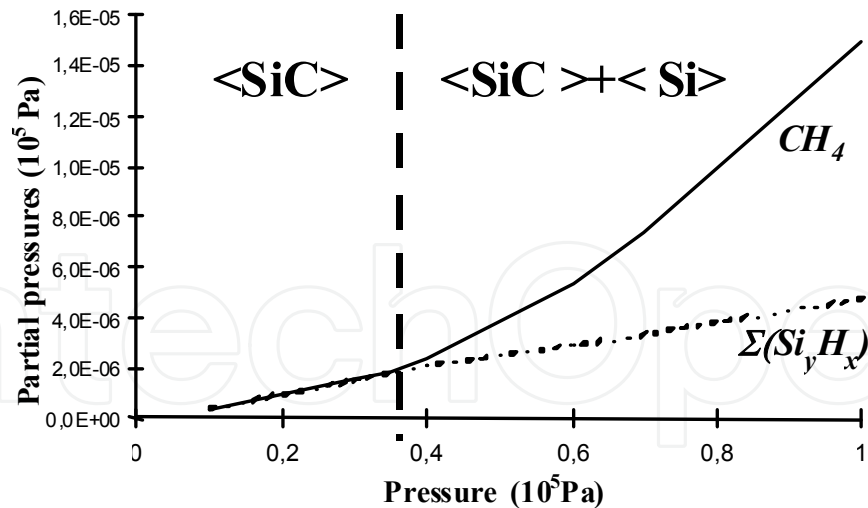


**Figure 3.** Heterogeneous equilibrium of the SiC(s) - H<sub>2</sub>(g) system at 1685K. Gaseous species created by the etching are represented as a function of the pressure [41].

### 3.3. Thermodynamic analysis of plasma etching processes for microelectronics

With the constant downscaling of Complementary Metal-Oxide-Semiconductor (CMOS) devices and the consequent replacement of SiO<sub>2</sub> many high-*k* gate materials such as Al<sub>2</sub>O<sub>3</sub>, La<sub>2</sub>O<sub>3</sub>, Ta<sub>2</sub>O<sub>5</sub>, TiO<sub>2</sub>, HfO<sub>2</sub>, ZrO<sub>2</sub> and Y<sub>2</sub>O<sub>3</sub> have been investigated. For each high-*k* material integration, the etch process has to be revisited.

In the case of the etching of HfO<sub>2</sub>, one of the main issues is the low volatility of halogenated based etch by-products [42].

Compared to SiO<sub>2</sub> halide based etching process, thermodynamic data shows that, Hf based etch by-products (HfCl<sub>4</sub>(g), HfBr<sub>4</sub>(g), HfF<sub>4</sub>(g)) are less volatile than Si etch by products (SiCl<sub>4</sub>(g), SiBr<sub>4</sub>(g), SiF<sub>4</sub>(g)) [43]. Therefore, for HfO<sub>2</sub>(s) etching, the choice of the halogenated based chemistry and substrate temperature are crucial parameters. In this work, thermodynamic studies have been carried out in the pressure (0.5 Pa) and temperature range (425 K to 625 K) conditions in order to select the most appropriate gas mixture and temperature leading to the formation of Hf and O based volatile products. Based on thermodynamic calculations in a closed system, the HfO<sub>2</sub>(s) etching process has been simulated.

With this thermodynamic analyses, it is possible to determine an etch chemistry leading to volatile compounds and to estimate an etch rate under pure chemical etching conditions. It should be noted that the thermodynamic approach does not take into account the ion bombardment of the plasma.

#### 3.3.1. Pure thermodynamic calculations of HfO<sub>2</sub> etching

For example, let's consider the etching of HfO<sub>2</sub>(s) in CCl<sub>4</sub>(g) plasma at 400 K and 0.5Pa. In such case, the thermodynamic system is composed by four elements Hf, O, C, and Cl. The thermodynamic calculation inputs are: each element of CCl<sub>4</sub>(g) (C and Cl atoms) with

HfO<sub>2</sub>(s) as a solid phase. The main gaseous species are CO<sub>2</sub>(g) and HfCl<sub>4</sub>(g) and the main condensed species are HfCl<sub>4</sub>(s) on HfO<sub>2</sub>(s) in a solid phase. There are other gaseous species in very low amount so that they can be neglected as (CO, Cl<sub>2</sub>, Cl). These results show that carbon and chlorine containing chemistries can lead to the etching of HfO<sub>2</sub>(s) by forming CO<sub>2</sub>(g) and HfCl<sub>4</sub>(g). Similar results have been obtained for the other halide chemistries CCl<sub>3</sub>F(g), CCl<sub>2</sub>F<sub>2</sub>(g), CCl<sub>3</sub>F(g), CCl<sub>4</sub>(g).

### 3.3.2. Thermodynamic analysis coupled to mass transport: evaluation of etching rate

To point out the more promising chemistry among the usually adopted halogens precursors, the etch rate has been estimated from the flow calculations of each gaseous and condensed species under open conditions assuming molecular flow and the validity of the Hertz-Knudsen relation [44].

For these processes operating at low pressure (<10 Pa), it is possible to associate the incident and emitted flows from a given surface to the equilibrium partial pressures [45].

These calculations are based on the effusion calculations principles from the gas kinetic theory.

For a gaseous species *e*, the total flow  $\Phi_e$  which is emitted from a vaporizing surface can be calculated according to the Hertz-Knudsen relation:

$$\Phi_e = \frac{p_e}{\sqrt{2\pi M_e RT}} \text{ mol / s.m}^2 \quad (25)$$

Where  $p_e$  et  $M_e$  are the partial pressure and molar mass of the species *e*, respectively.

For each etched or deposited element *i*, there is equality between the incident flow and the emitted or produced from reactions flows:

$$\Phi_i(\text{incident}) = \Phi_i(\text{emitted}) + \Phi_i(\text{condensed}) \quad (26)$$

on the deposited or etched surface

For example, in the case of HfO<sub>2</sub>(s) etching by CHCl<sub>3</sub>(g) with Ar(g), the system is Hf, O, C, H, Cl, Ar

For the previous thermodynamic calculations (HfO<sub>2</sub>(s) and CHCl<sub>3</sub>(g)) the major species at equilibrium are:

- CO<sub>2</sub>(g), HCl(g), HfCl<sub>4</sub>(g), Ar(g) in the gaseous phase
- C(s), HfO<sub>2</sub>(s), HfCl<sub>4</sub>(s) in the solid phase

for a temperature of 300 K and a pressure of 5 Pa.

The flow equations are in this case (principle of mass conservation) :

- Flow of incident C = flow of evaporated C + flow of condensed C:

$$\frac{1}{\sqrt{2\pi \cdot R \cdot T}} \frac{P_{CO_2}}{\sqrt{M_{CO_2}}} + F(C(s)) = \phi(CHCl_3(g)) \quad (27)$$

- Flow of incident H = flow of evaporated H :

$$\frac{1}{\sqrt{2\pi \cdot R \cdot T}} \frac{P_{HCl}}{\sqrt{M_{HCl}}} = \phi(CHCl_3(g)) \quad (28)$$

- Flow of incident Cl = flow of evaporated Cl + flow of condensed Cl :

$$\frac{1}{\sqrt{2\pi \cdot R \cdot T}} \left( \frac{P_{HCl}}{\sqrt{M_{HCl}}} + 4 \cdot \frac{P_{HfCl_4}}{\sqrt{M_{HfCl_4}}} \right) + F(HfCl_4(s)) = 3 \cdot \phi(CHCl_3(g)) \quad (29)$$

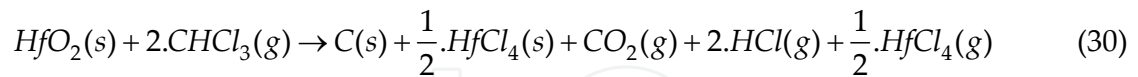
with  $F(.(s))$  the flow in solid phase species and  $\phi(CHCl_3(g)) = \frac{p_{CHCl_3}^0}{\sqrt{2\pi \cdot M_{CHCl_3} \cdot R \cdot T_0}}$  (To the temperature at the gases inlet and  $p_{CHCl_3}^0$  the inlet partial pressure).

So five unknowns are obtained:  $P_{CO_2}, F(C(s)), P_{HCl}, P_{HfCl_4}, F(HfCl_4(s))$

To be able to solve this system, five equations are needed. Already, three equations with these ones of flow exist. For the both missing, it's enough to consider:

The equation of total pressure:  $P_{CO_2} + P_{HCl} + P_{HfCl_4} + P_{Ar} = P_{totale}$

And the value of the equilibrium constant for the assessment of mass equation of the system, the fifth global equation is supplied by:



the equilibrium constant of this equation is :

$$K_p = \frac{P_{CO_2} \cdot P_{HfCl_4}^{\frac{1}{2}} \cdot P_{HCl}^2}{P_{CHCl_3}^2} \quad (31)$$

$$\text{with : } \begin{cases} P_{CO_2} = x_1 \\ P_{HCl} = x_2 \\ P_{HfCl_4} = x_3 \\ F(C(s)) = x_4 \\ F(HfCl_4(s)) = x_5 \end{cases} \quad (32)$$

The system of five equations and five unknowns is obtained:

$$\left\{ \begin{array}{l} \frac{1}{\sqrt{2\pi \cdot R \cdot T}} \frac{x_1}{\sqrt{M_{CO_2}}} + x_4 = \phi(CHCl_3) \\ \frac{1}{\sqrt{2\pi \cdot R \cdot T}} \frac{x_2}{\sqrt{M_{HCl}}} = \phi(CHCl_3) \\ \frac{1}{\sqrt{2\pi \cdot R \cdot T}} \left( \frac{x_2}{\sqrt{M_{HCl}}} + 4 \cdot \frac{x_3}{\sqrt{M_{HfCl_4}}} \right) + x_5 = 3 \cdot \phi(CHCl_3) \\ x_1 + x_2 + x_3 + P_{Ar} = P_{Totale} \\ \frac{x_1 \cdot x_3^2 \cdot x_2^2}{P_{CHCl_3}^2} = K_p \end{array} \right. \quad (33)$$

The partial pressures of the main species are obtained. To determine the etch rate, it is needed to use the calculated values for the pressures of the gases containing the elements of material to etch.

In our example, the following gases  $CO_2(g)$  and  $HfCl_4(g)$  are considered.

The theoretical etch rate ER is given by the lowest value between:

ER = flow  $HfCl_4(g)$ .molar volume  $HfCl_4(g)$  or flow  $CO_2(g)$ .molar volume  $CO_2(g)$  (in m/s)

Where:

$$Flow_{CO_2} = \frac{N}{\sqrt{2\pi \cdot R \cdot T}} \cdot \frac{P_{CO_2}}{\sqrt{M_{CO_2}}} \quad (34)$$

and

$$Flow_{HfCl_4} = \frac{N}{\sqrt{2\pi \cdot R \cdot T}} \cdot \frac{P_{HfCl_4}}{\sqrt{M_{HfCl_4}}} \quad (\text{in molecules / s.m}^2) \quad (35)$$

with  $P_{CO_2}$  and  $P_{HfCl_4}$  determined by the resolution of the mathematical system and N the Avogadro number, P in Pa and M in kg.

Figure 4 shows the evolution of the calculated  $HfO_2(s)$  etch rate as a function of temperature for different F/Cl ratios in  $CCl_xF_y(g)$  based chemistries. The etch rate is lower when the F/Cl ratio increases in the gas mixture at temperature higher than 400 K. The decrease in the etch rate is explained by the non volatility of  $HfF_4(g)$  in the investigated temperature range.

### 3.3.3. Conclusions

From these results, thermodynamic studies predict that a chlorocarbon gas mixture -such as  $\text{CCl}_4$  -seems to be the most promising chemistry to etch  $\text{HfO}_2(\text{s})$  under pure chemical etching conditions.

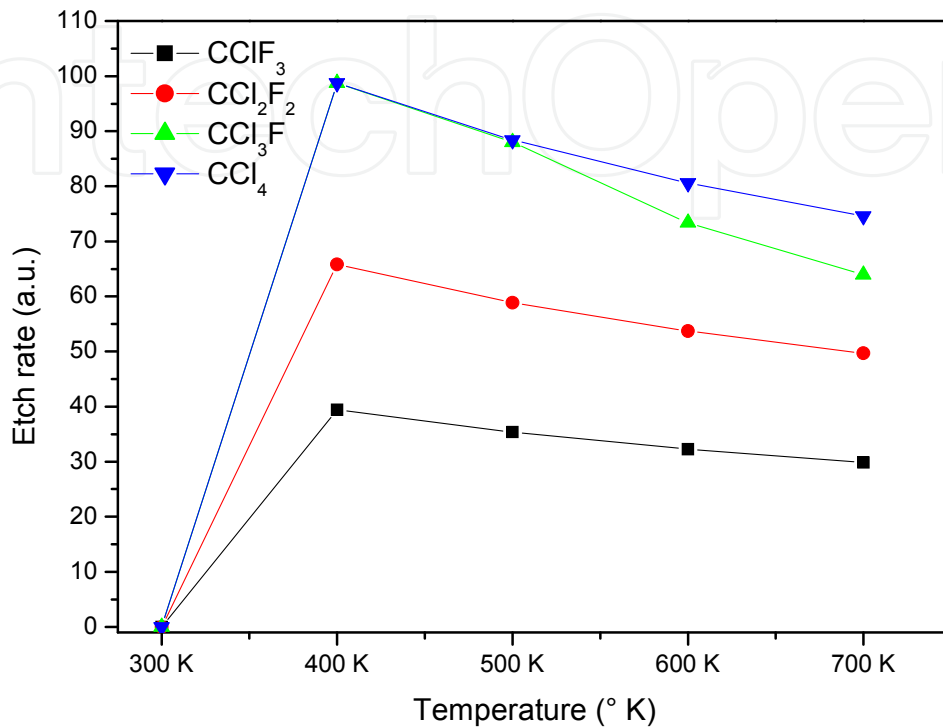


**Figure 4.** Evolution of the thermodynamically calculated  $\text{HfO}_2(\text{s})$  etch rate as a function of F-Cl ratio in  $\text{CCl}_x\text{F}_y(\text{g})$  based chemistries.

### 3.4. Optics: $\text{SiO}_2$ PVD deposition

From optics applications, the example of the evaporation/condensation process to obtain  $\text{SiO}_2$  films is chosen. In that process, the surface of the evaporating source is heated by electronic bombardment, while the substrate is held at low temperature.

The control and the reproducibility of this type of process is based on the following points:

- Stability of the source with time (chemical composition, morphology of surface of the evaporating zone)
- Temperature and surface of the evaporated area (what is linked to the parameters of the electronic bombardment).

The object of this study is to simulate the evaporation of a source of glassy silica with the aim of depositing  $\text{SiO}_2$ . The heated zone is about  $3\text{-}7\text{ cm}^2$ , the reactor has a volume about  $1\text{ m}^3$ , the substrate is located at  $1\text{ m}$  from the source.

The first paragraph is dedicated to the pure thermodynamic simulations to determine the major species originated from the evaporation. In the second one, the calculations of the

flows of evaporation at equilibrium as well as exchanged flows between source and substrate surfaces are presented.

### 3.4.1. Pure thermodynamic calculations of $\text{SiO}_2$ evaporation

The thermodynamic simulations corresponding to the  $\text{SiO}_2(\text{s})$  evaporation are realized by considering an excess of solid  $\text{SiO}_2(\text{s})$  at a given temperature, in a constant volume. The range of tested temperature is 1600 - 2500 K. The results of the simulation indicate that the only solid present at equilibrium is  $\text{SiO}_2(\text{s})$  and that there is no formation of solid silicon.

In the range of selected temperature, the evaporation of the silica is thus congruent (the ratio of the quantity of silicon and oxygen produced in the gaseous form is equal to 2). Figure 5 presents the nature and the partial pressures of the gaseous species formed at equilibrium.

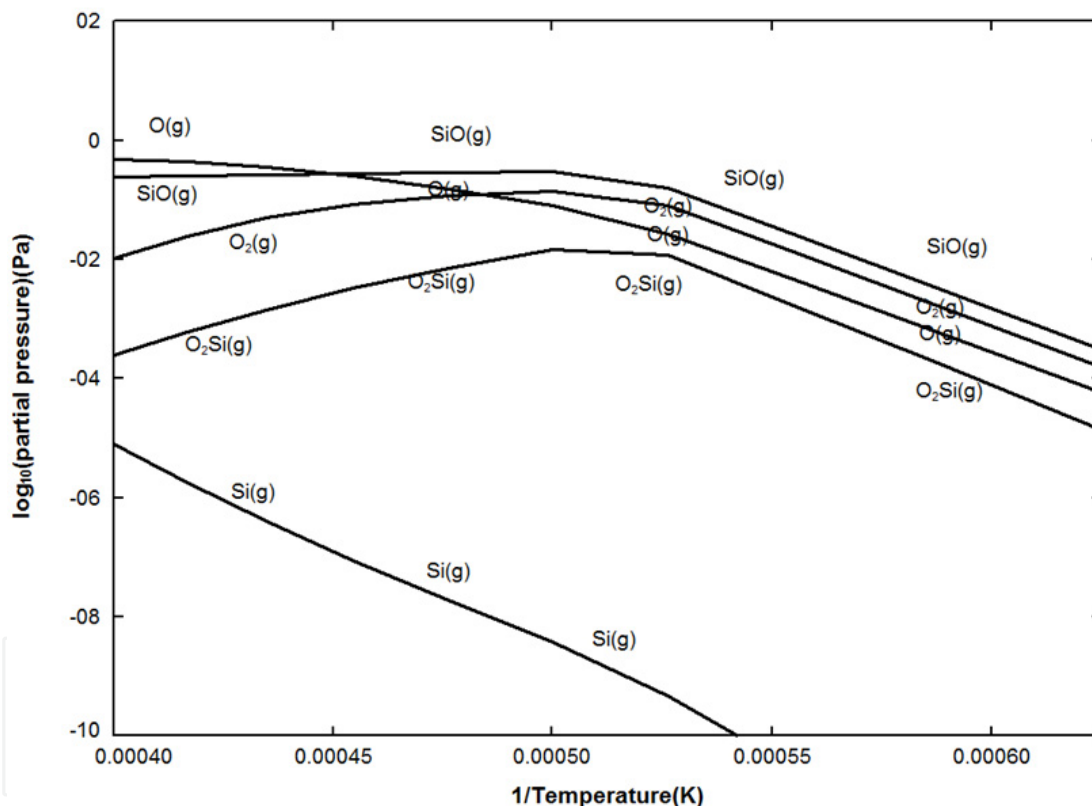
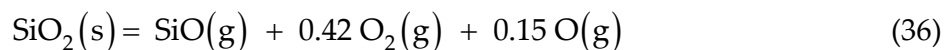


**Figure 5.** Calculated partial pressures for  $\text{SiO}_2$  vaporization.

The major species in this range of temperature are  $\text{SiO}(\text{g})$ ,  $\text{O}_2(\text{g})$ ,  $\text{O}(\text{g})$  and  $\text{SiO}_2(\text{g})$ , with trace of  $\text{Si}(\text{g})$ . It can be noted that the mainly evaporated species is not  $\text{SiO}_2(\text{g})$  as it could be believed to justify the stoichiometric composition of the deposits. From the results of the molar fractions calculated for various species, the gas phase reaction which takes place is globally the following:



These curves show that the evaporated material quantity and consequently the evaporation rate increases with temperature. That explains the best results obtained with sources carried beyond their melting point (besides the higher quality of the surface with regard to a solid source).

The calculated total pressure above silica is represented on the figure 5.

For the temperatures of evaporation above 1600 K, the total pressure over the silica is superior to 0.1 Pa. If the total pressure is fixed to a lower value, there is then complete consumption of the quantity of silica carried at the evaporation temperature from a thermodynamic point of view.

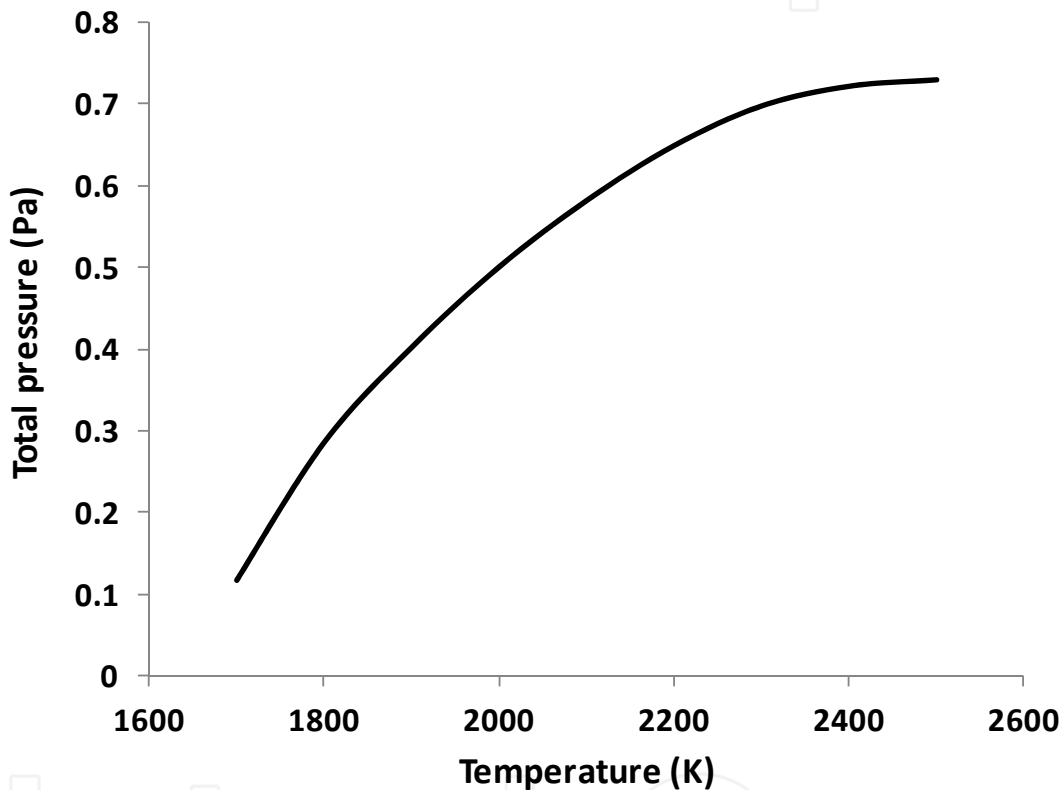


**Figure 6.** Calculated total pressure for SiO<sub>2</sub>(s) vaporization

### 3.4.2. Thermodynamic analysis coupled to mass transport: evaluation of deposition rate

The evaporation flows of the gaseous species originating from the SiO<sub>2</sub>(s) evaporation should respect the congruent vaporization relation (ratio Si/O in the gaseous phase = 2), demonstrated by the previous approach.

$$2 * \Phi_{O_2} + \Phi_{SiO} + \Phi_O + 2 * \Phi_{Si_2O_2} + 2 * \Phi_{SiO_2} = \Phi_{Si} + 2 * \Phi_{SiO} + \Phi_O + 4 * \Phi_{Si_2O_2} + 2 * \Phi_{SiO_2} \quad (37)$$

where  $\Phi_e$  is the molecular flow of the species  $e$ , according to equation (25).

As illustrated by the previous etching case, it is possible to calculate all the species partial pressures ( $p_e$ ) which verify the equation (37).

From the calculated flows from equation (37), the molar volume of SiO<sub>2</sub>(s), the reactor geometry, and the temperature conditions on the surface, it is possible to estimate the growth rate and the deposition profile (Figure 7). The growth rate on the substrate is given from the exchanged flows between the two surfaces source and substrate, from basic assumptions of molecular flows.

With coaxial source and substrate, the exchanged flow between the  $r_0$  radius source and  $r_1$ , radius substrate, separated by a distance  $h$  is given by the relation (38).

$$\Phi_e = \frac{\alpha_e p_e}{\sqrt{2\pi M_e RT}} * \frac{\pi}{2} * [h^2 + r_0^2 + r_1^2 - \sqrt{(h^2 + r_0^2 + r_1^2)^2 - 4 * r_0^2 r_1^2}] \text{ mol / s.m}^2 \quad (38)$$

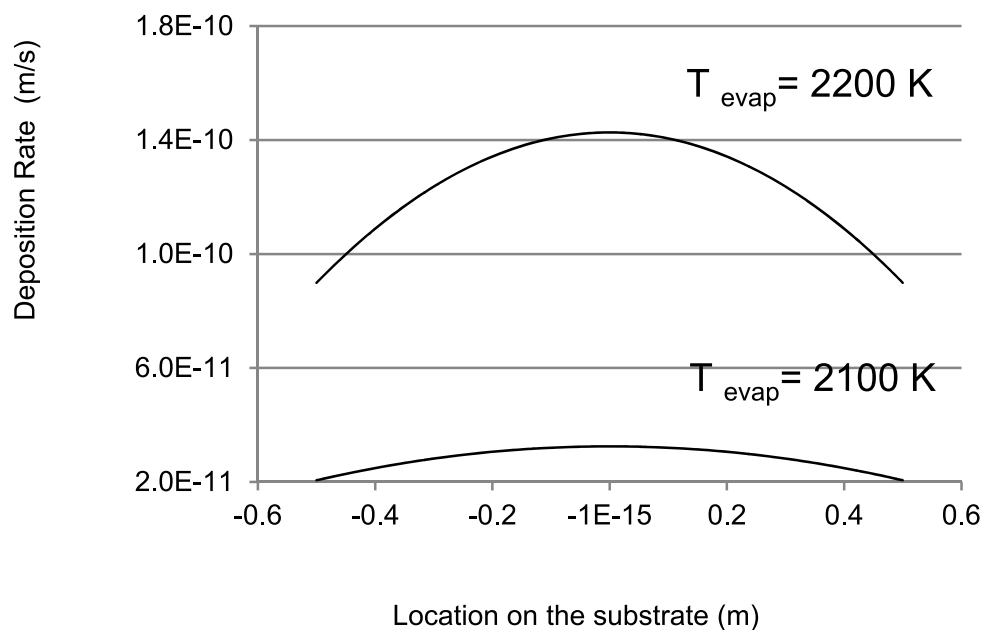


**Figure 7.** Deposition profile vs deposition temperature for two evaporation temperatures; Substrate radius  $r_0=0.5$  m; evaporating source surface=  $3\text{cm}^2$ ,  $h=1$  m

The results of the simulations are the same order as the obtained experimental values.

### 3.4.3. Conclusions

The simulations of the evaporation of SiO<sub>2</sub>(s) show that it is congruent and that there is thus no evolution of the load in time. The mainly produced gaseous species are SiO(g), O<sub>2</sub>(g), and O(g). Their proportions remain constant but their quantities increase with the temperature of evaporation. Simulations of the evaporation/condensation process provide good estimations of the deposition rate.

## 4. Conclusions

This review illustrates the interest to operate a priori an thermodynamic approach to determine the feasibility and optimize a fabrication process, specially gas-solid fabrication

process. Kinetic approaches will give rise to more realistic simulations but are often difficult to implement, for lack of reliable information. The classic pure thermodynamic can provide useful information. It can be the only approach in the case of complex chemical systems for which few kinetic data are available. To take into account the dynamic character of the processes, the approaches mixing thermodynamics simulations and calculations of exchanged flows are possible. In every case, the methodology has to contain continuous comparisons between experimental results and simulations.

## Author details

Elisabeth Blanquet and Ioana Nuta

Laboratory "Science et Ingénierie des Matériaux et Procédés (SIMaP)"

Grenoble INP/CNRS/UJF, Saint Martin d'Hères, France

## Acknowledgement

This paper was inspired by the collaborative works with the colleagues of the SIMaP (Laboratoire de Science et Ingénierie des Matériaux et Procédés): Jean-Noël Barbier, Claude Bernard, Christian Chatillon, Alexander Pisch, Arnaud Mantoux, Raphaël Boichot, Michel Pons.

## 5. References

- [1] Cheynet, B., Chevalier, P.-Y., Fischer, E. (2002) Thermosuite. *Calphad*. 26: 167-174.
- [2] Hack, K. (1996) The SGTE casebook: thermodynamics at work. Scientific Group Thermodata Europe and Institute of Materials.
- [3] McBride, B. J., Zehe, M. J., Gordon, S. (2002) NASA Glenn Coefficients for Calculating Thermodynamic Properties of Individual Species NASA.
- [4] Miedema, A., De Chatel, P., De Boer, F. R. (1980) Cohesion in alloys—fundamentals of a semi-empirical model. *Physica B+ C*. 100: 1-28.
- [5] Hansen, M., Anderko, K. (1958) Constitution of Binary Alloys, Metallurgy and Metallurgical Engineering Series. New York: McGraw-Hill
- [6] Elliott, R. (1965) Constitution of Binary Alloys, First Supplement. New York: McGraw-Hill.
- [7] Massalski, T. B., Okamoto, H., Subramanian, P. R., Kacprazac, L. (1990) Binary alloy phase diagrams. Ohio: ASM International, Materials Park.
- [8] Villars, P., Prince, A., Okamoto, H. (1995) Handbook of Ternary Alloy Phase Diagrams. Ohio: ASM International, Materials Park.
- [9] Chase, M. (1998) NIST-JANAF thermochemical tables. Washington, D.C. and Woodbury, N.Y.: American Chemical Society.
- [10] Barin, I. (1993) Thermochemical data of pure substances. New York: VCH.
- [11] Gurvich, L. V., Veyts, I., Alcock, C. B. (1990) Thermodynamic Properties of Individual Substances. New York: Hemisphere Pub.

- [12] SGTE, S. G. T. E. 38402 Saint Martin d'Herès, France.
- [13] GTT-Technologies. 52134 Herzogenrath, Germany.
- [14] Bale, C., Chartrand, P., Degterov, S., Eriksson, G., Hack, K., Ben Mahfoud, R., Melançon, J., Pelton, A., Petersen, S. (2002) FactSage thermochemical software and databases. *Calphad*. 26: 189-228.
- [15] Belov, G. V., Iorish, V. S., Yungman, V. S. (1999) IVTANTHERMO for Windows--database on thermodynamic properties and related software. *Calphad*. 23: 173-180.
- [16] Warnatz, J. (1984) *Combustion chemistry*. New York.
- [17] (2005) NIST Chemistry WebBook, NIST Standard Reference Database. Gaithersburg MD.
- [18] Smith, W. R., Missen, R. W. (1982) *Chemical reaction equilibrium analysis: theory and algorithms*. New York: Wiley
- [19] Barbier, J. N., Bernard, C. (1986). In *Calphad XV*. Fulmer Grange, U.K.
- [20] Davies, R., Dinsdale, A., Gisby, J., Robinson, J., Martin, S. (2002) MTDATA--thermodynamic and phase equilibrium software from the National Physical Laboratory. *Calphad*. 26: 229-271.
- [21] Sundman, B., Jansson, B., Andersson, J. O. (1985) The thermo-calc databank system. *Calphad*. 9: 153-190.
- [22] Thomas, N., Suryanarayana, P., Blanquet, E., Vahlas, C., Madar, R., Bernard, C. (1993) LPCVD WSi<sub>2</sub> Films Using Tungsten Chlorides and Silane. *Journal of the Electrochemical Society*. 140: 475-484.
- [23] Bernard, C., Pons, M., Blanquet, E., Madar, R. (1999) Computer simulations from thermodynamic data: Materials productions and development--Thermodynamic Calculations as the Basis for CVD Production of Silicide Coatings. *MRS Bulletin--Materials Research Society*. 24: 27-31.
- [24] Pons, M., Bernard, C., Blanquet, E., Madar, R. (2000) Combined thermodynamic and mass transport modeling for material processing from the vapor phase. *Thin Solid Films*. 365: 264-274.
- [25] Brize, V., Prieur, T., Violet, P., Artaud, L., Berthome, G., Blanquet, E., Boichot, R., Coindeau, S., Doisneau, B., Farcy, A., Mantoux, A., Nuta, I., Pons, M., Volpi, F. (2011) Developments of TaN ALD Process for 3D Conformal Coatings. *Chem. Vapor Depos.* 17: 284-295.
- [26] Violet, P., Blanquet, E., Monnier, D., Nuta, I., Chatillon, C. (2009) Experimental thermodynamics for the evaluation of ALD growth processes. *Surface and Coatings Technology*. 204: 882-886.
- [27] Violet, P., Nuta, I., Chatillon, C., Blanquet, E. (2007) Knudsen cell mass spectrometry applied to the investigation of organometallic precursors vapours. *Surface and Coatings Technology*. 201: 8813-8817.
- [28] Dinsdale, A. (1991) SGTE data for pure elements. *Calphad*. 15: 317-425.
- [29] Violet, P., Nuta, I., Artaud, L., Collas, H., Blanquet, E., Chatillon, C. (2009) A special reactor coupled with a high-temperature mass spectrometer for the investigation of the vaporization and cracking of organometallic compounds. *Rapid Communications in Mass Spectrometry*. 23: 793-800.

- [30] Di Cioccio, L., Billon, T. (2002) Advances in SiC materials and technology for Schottky diode applications. In *Silicon Carbide and Related Materials 2001, Pts 1 and 2, Proceedings*, eds. Yoshida, S., Nishino, S., Harima, H. & Kimoto, T., 1119-1124.
- [31] Matsunami, H. (2000) An overview of SiC growth. 125-130. *Trans Tech Publ.*
- [32] Pons, M., Blanquet, E., Dedulle, J., Garcon, I., Madar, R., Bernard, C. (1996) Thermodynamic heat transfer and mass transport modeling of the sublimation growth of silicon carbide crystals. *Journal of the Electrochemical Society*. 143: 3727-3735.
- [33] Pons, M., Anikin, M., Chourou, K., Dedulle, J., Madar, R., Blanquet, E., Pisch, A., Bernard, C., Grosse, P., Faure, C. (1999) State of the art in the modelling of SiC sublimation growth. *Materials Science and Engineering: B*. 61: 18-28.
- [34] Pons, M., Baillet, F., Blanquet, E., Pernot, E., Madar, R., Chaussende, D., Mermoux, M., Di Coccio, L., Ferret, P., Feuillet, G., Faure, C., Billon, T. (2003) Vapor phase techniques for the fabrication of homoepitaxial layers of silicon carbide: process modeling and characterization. *Applied Surface Science*. 212-213: 177-183.
- [35] Bernard, C., Blanquet, E., Pons, M. (2007) Chemical vapor deposition of thin films and coatings: Evaluation and process modeling. *Surface and Coatings Technology*. 202: 790-797.
- [36] Hallin, C., Ivanov, I.G., Henry, A., Egilsson, T., Kordina, O., and Janzen, E. 1998, *J. Crystal Growth*, 183, 1-2, 163.
- [37] Allendorf, M. D., Melius, C. F. (1992) Theoretical study of the thermochemistry of molecules in the silicon-carbon-hydrogen system. *The Journal of Physical Chemistry*. 96: 428-437.
- [38] Allendorf, M. D., Melius, C. F. (1993) Theoretical study of thermochemistry of molecules in the silicon-carbon-chlorine-hydrogen system. *The Journal of Physical Chemistry*. 97: 720-728.
- [39] Rocabois, P., Chatillon, C., Bernard, C. (1995) Thermodynamics of the Si-C system I. mass spectrometry studies of the condensed phases at high temperature. *High Temperatures. High Pressures*. 27: 3-23.
- [40] Rocabois, P., Chatillon, C., Bernard, C., Genet, F. (1995) Thermodynamics of the Si-C system II. Mass spectrometric determination of the enthalpies of formation of molecules in the gaseous phase. *High Temperatures. High Pressures*. 27: 25-39.
- [41] Neyret, E., Di Cioccio, L., Blanquet, E., Raffy, C., Pudda, C., Billon, T., J., C. (2000) SiC in situ pre-growth etching : a thermodynamic study. In *Int. Conf. on Silicon Carbide and Related Materials*, 1041-1044. *Materials Science Forum*.
- [42] Helot, M., Chevolleau, T., Vallier, L., Joubert, O., Blanquet, E., Pisch, A., Mangiagalli, P., Lill, T. (2006) Plasma etching of HfO at elevated temperatures in chlorine-based chemistry. *Journal of Vacuum Science & Technology A: Vacuum, Surfaces, and Films*. 24: 30.
- [43] Chen, J., Yoo, W. J., Tan, Z. Y. L., Wang, Y., Chan, D. S. H. (2004) Investigation of etching properties of HfO based high-K dielectrics using inductively coupled plasma. *Journal of Vacuum Science & Technology A: Vacuum, Surfaces, and Films*. 22: 1552-1558.

- [44] Dumas, L., Chatillon, C., Quesnel, E. (2001) Thermodynamic calculations of congruent vaporization and interactions with residual water during magnesium fluoride vacuum deposition. *Journal of Crystal Growth*. 222: 215-234.
- [45] Shen, J.-y., Chatillon, C. (1990) Thermodynamic calculations of congruent vaporization in III–V systems; Applications to the In-As, Ga-As and Ga-In-As systems. *Journal of Crystal Growth*. 106: 543-552.

IntechOpen

IntechOpen